Spatial variability of carbon monoxide in Venus' mesosphere from Venus Express/Visible and Infrared Thermal Imaging Spectrometer measurements

Patrick G. J. Irwin, Remco de Kok, Alberto Negrao, Constantine C. C. Tsang, Colin F. Wilson, Pierre Drossart, Giuseppe Piccioni, Davide Grassi, Frederic W. Taylor

Spatial variability of carbon monoxide in Venus' mesosphere from Venus Express/Visible and Infrared Thermal Imaging Spectrometer measurements

P. G. J. Irwin,[1] R. de Kok,[1] A. Negrão,[2] C. C. C. Tsang,[1] C. F. Wilson,[1] P. Drossart,[3] G. Piccioni,[4] D. Grassi,[2] and F. W. Taylor[1]

Received 1 February 2008; revised 16 April 2008; accepted 5 May 2008; published 23 July 2008.

[1] Observations of Venus' mesosphere by the Visible and Infrared Thermal Imaging Spectrometer (VIRTIS)-M instrument of Venus Express have been used to investigate the spatial distribution of CO above Venus' nightside cloud tops by fitting the CO absorption in the (1–0) CO band around 4.7 μm. We find little spatial variation in the abundance of CO at midlatitudes, with a retrieved abundance of approximately 40 ± 10 ppm just above the cloud tops between 65 and 70 km altitude. Unfortunately, we find it very difficult to constrain the abundance of CO in the cold polar collar, centered at about 70°S, as the retrieved temperature structure in the CO line-forming region masks the absorption lines. However, there is a possibility that CO increases toward the poles, as we detect a significant signature of high levels of CO over Venus' south polar dipole feature in all the observations analyzed so far. To constrain the abundance of CO more closely will require the analysis of higher-resolution VIRTIS-H observations. In addition, limb observations would greatly help to resolve any possible temperature/cloud ambiguities and allow us to assess vertical variations in the abundance of CO.

Citation: Irwin, P. G. J., R. de Kok, A. Negrão, C. C. C. Tsang, C. F. Wilson, P. Drossart, G. Piccioni, D. Grassi, and F. W. Taylor (2008), Spatial variability of carbon monoxide in Venus' mesosphere from Venus Express/Visible and Infrared Thermal Imaging Spectrometer measurements, *J. Geophys. Res.*, *113*, E00B01, doi:10.1029/2008JE003093.

1. Introduction

[2] Carbon monoxide is produced at equatorial and midlatitudes in the dayside upper atmosphere of Venus by UV photolysis ($\lambda < 224$ nm) of CO_2 [*von Zahn et al.*, 1983; *Huebner et al.*, 1992]. It is thought to be transported toward the poles by the planet's Hadley cell circulation, where it is then subducted and recombined with O near Venus' hot surface, perhaps via sink reactions with either carbonyl sulfide (OCS) [*Pollack et al.*, 1993], or S_2 [*Hong and Fegley*, 1997]. It is thus expected that the volume mixing ratio of CO decreases as we move deeper into the atmosphere, both owing to such recombination reactions and also owing to the CO-rich air from high altitudes being steadily diluted by mixing with CO-poor air at lower altitudes. Superimposed on this meridional circulation, CO is also rapidly transported longitudinally in Venus' upper atmosphere by Venus' strong zonal winds at these pressure levels. Thus, even though it is produced on Venus' dayside, CO is expected to be quickly transported to Venus' nightside where it can be detected at thermal-IR wavelengths in the (1–0) CO band around 4.7 μm.

[3] Existing observations of CO prior to the arrival of the Venus Express mission at Venus in 2006 are reviewed by *de Bergh et al.* [2006] and issues concerning the modeling of the distribution of CO are reviewed by *Mills and Allen* [2007]. The abundance of CO at high altitudes (around 100 km altitude) is estimated from observations at millimeter [e.g., *Clancy and Muhleman*, 1991; *Gurwell et al.*, 1995] and submillimeter [e.g., *Clancy et al.*, 2003] wavelengths to be highly variable and of the order of 100–1000 ppm, while deeper in the atmosphere, the CO abundance has been inferred from measurements of the near-infrared emission from Venus' night side. *Bézard et al.* [1990] and *Pollack et al.* [1993] used data from the Canada France Hawaii Telescope to infer mean values of 40 ppm and 23 ± 5 ppm at 36 km respectively, with *Pollack et al.* [1993] also estimating that the abundance of CO increased with height at a rate of 1.20 ± 0.45 ppm/km. These observations roughly coincided with the flyby of Venus of NASA's Galileo spacecraft, on its way to Jupiter. During the encounter, the NIMS (Near-Infrared Mapping Spectrometer) instrument made the first space-based observations of Venus' night side near-infrared emission and *Collard et al.* [1993] used these data to determine the latitudinal distribution of CO in the deep atmosphere, finding that it increased toward the poles with a maximum abundance at approximately 60°N.

[1] Atmospheric, Oceanic, and Planetary Physics, Clarendon Laboratory, University of Oxford, Oxford, UK.
[2] INAF-IFSI, Rome, Italy.
[3] LESIA, Observatoire de Paris, Meudon, France.
[4] INAF-IASF, Rome, Italy.

0148-0227/08/2008JE003093

Table 1. Summary of Observations Used in This Study[a]

Name	Orbit	Date	Start Time, UT	End Time, UT	n_λ	n_s	n_l	t_{exp} (s)
VI0029_06	29	19 May 2006	1658	1708	432	256	253	0.36
VI0029_07	29	19 May 2006	1713	1724	432	256	254	0.36
VI0029_08	29	19 May 2006	1729	1740	432	256	254	0.36
VI0038_00	38	28 May 2006	1641	1651	432	256	228	0.36
VI0067_00	67	26 June 2006	1449	1454	432	256	126	0.36
VI0067_01	67	26 June 2006	1503	1509	432	256	126	0.36
VI0067_02	67	26 June 2006	1517	1523	432	256	126	0.36
VI0067_03	67	26 June 2006	1534	1540	432	256	126	0.36
VI0067_04	67	26 June 2006	1542	1548	432	256	126	0.36
VI0067_05	67	26 June 2006	1553	1559	432	256	126	0.36

[a]Here n_λ is the number of wavelengths, n_s is the number of spatial samples, and n_l is the number of spatial lines; t_{exp} is the exposure time.

[4] New observations of Venus' near-infrared emission have been made by the VIRTIS instrument on Venus Express and these data have been used to investigate further the spatial variation of CO in the deep atmosphere by C. C. C. Tsang et al. (Tropospheric Carbon Monoxide Concentrations and Variability on Venus from Venus Express/VIRTIS-M Observations, submitted to *Journal of Geophysical Research*, 2008) and E. Marcq et al. (A latitudinal survey of CO, OCS, H_2O and SO_2 in the lower atmosphere of Venus: Spectroscopic studies using VIRTIS-H, submitted to Journal of Geophysical Research, 2008). Higher in the atmosphere, SPICAV/SOIR UV data have been used to determine the vertical distribution of CO above 60 km, finding values of 10–20 ppm at midlatitudes at an altitude of 70 km, decreasing to ~4 ppm at 90 km, and then increasing rapidly at higher altitudes [*Svedhem et al.*, 2007; *Bertaux et al.*, 2007].

2. Measurements

[5] The Venus Express spacecraft was launched on a Soyuz-Fregat rocket from Baikonur, Kazakhstan on 9 November 2005 and went into a near-polar 24 h orbit about Venus on 11 April 2006, where it will remain until at least May 2009.

[6] The spacecraft carries a number of remote sensing instruments including VIRTIS (Visible and Infrared Thermal Imaging Spectrometer), which covers the wavelength range 0.27 to 5.19 μm. The VIRTIS instrument is split into two main subsystems, the high-resolution subsystem, VIRTIS-H, and the mapper subsystem, VIRTIS-M. The VIRTIS-H subsystem is an Echelle spectrometer covering the 1.84 to 4.99 μm range at a spectral resolution of 0.001 μm, with an instantaneous field of view (IFOV) of 0.45 × 2.25 mrad. The VIRTIS-M subsystem, has an IFOV of 0.25 × 64 mrad sampled by 256 rows of a CCD array, which can be scanned to generate an image covering 64 × 64 mrad with an angular resolution of 0.25 × 0.25 mrad. At an apogee of 66,000 km, Venus' disk extends approximately 180 mrad and thus a complete image of Venus' disk may be generated by mosaicking 3 × 3 VIRTIS-M observations. The VIRTIS-M subsystem is itself split into two components: one component covers the 0.27 to 1.0 μm wavelength range with a spectral resolution of 0.002 μm, while an infrared component covers the 1.05 to 5.19 μm range at a lower spectral resolution of 0.01 μm.

[7] To investigate the distribution of CO in Venus' mesosphere we analyzed VIRTIS spectra from 4–5 μm. In this spectral range, there is a strong CO_2 absorption band at 4.3 μm and a weaker one at 4.8 μm, with the (1–0) absorption band of CO observable at around 4.7 μm. No other gases have a significant contribution in this range. At other wavelengths where gas absorption becomes negligible, the absorption of the upper cloud decks becomes important. Day side observations at these wavelengths are considerably complicated by reflected sunlight from the cloud tops and so we chose to concentrate upon VIRTIS-M night side observations where only thermal emission is important, and for which there exist several wide area maps from the south pole to the equator. We chose two sets of observations in particular, VI0029 and VI0067, whose characteristics are summarized in Table 1. These mapping observations were chosen because, at the time of writing, they covered the largest area and had the longest integration time, and consequently best signal-to-noise ratio. The signal-to-noise ratio of these spectra typically varies from about 1.0 in the center of the strong CO_2 band at 4.3 μm to roughly 40 where the radiance is greatest, near 4.9 μm. To improve the signal-to-noise ratio, the 4.0–4.95 μm spectra from the data 'cubes' sampling Venus' night side for these orbits (six cubes for VI0067 and three for VI0029) were averaged into 20 × 20 pixel boxes and stepped by 10 pixels in each direction to achieve Nyquist sampling. The areas covered by both sets of observations are shown in Figure 1. The error on the spectral points was set to either the NESR/$\sqrt{n}$ or the variance of the measured points divided by $\sqrt{n}$, whichever was larger, where n is the number of points averaged in a single bin and NESR is the noise equivalent spectral radiance.

[8] We also searched the measured data set for VIRTIS-M limb-sounding observations of Venus' night side, but at the time of writing could only identify one suitable observation, which was of the equatorial region and had insufficient vertical sampling to improve upon what could be extracted from the VIRTIS-M nadir observations.

3. Retrieval Model

[9] To analyze the recorded spectra, we used the NEMESIS correlated-*k* radiative transfer and retrieval model [*Irwin et al.*, 2008], which has been successfully applied to numerous planetary remote sensing missions, and has also been used by Tsang et al. (submitted manuscript, 2008) to determine the variability of CO in Venus' deep atmosphere. The NEMESIS retrieval code is based upon the optimal estimation formalism of *Rodgers* [2000], which assumes that a good knowledge exists of the expected

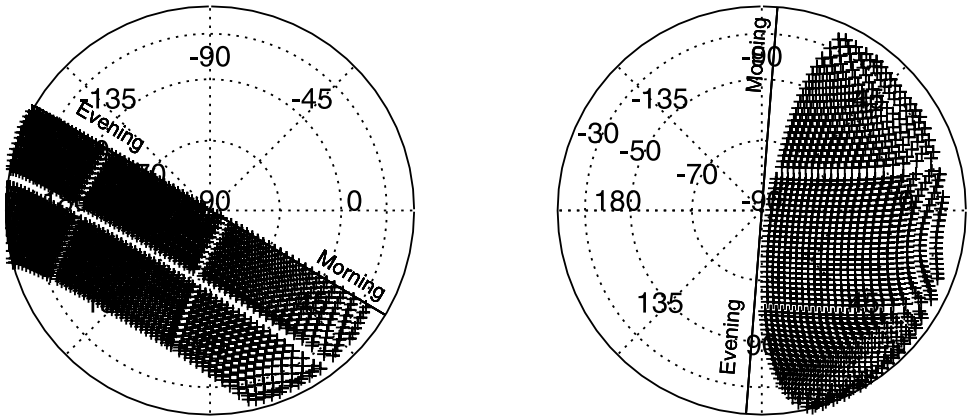

Figure 1. Sampling of Venus' southern hemisphere by the Venus Express/VIRTIS (left) VI0067 observations and (right) VI0029 observations.

variation in the retrieved parameters from other sources. Such a situation does not exist in this case and hence the a priori guessed profiles and covariance matrices are instead tuned to provide a reasonable balance between precision and vertical smoothing, in the manner of the constrained linear inversion technique [*Conrath et al.*, 1998; *Hanel et al.*, 2003], as described by *Irwin et al.* [2008].

[10] To use the model, *k*-distribution tables were first generated with VIRTIS-M resolution from line data for the different spectrally active gases in this spectral and pressure region. We used line data from the HITRAN 2004 database [*Rothman et al.*, 2005] with a Voigt line shape for all gases except CO_2, for which we used a sub-Lorentzian line shape of *Tonkov et al.* [1996] with a cutoff at 150 cm^{-1} from the line centers. Although this line shape was originally developed for analyzing spectra at 2.3 μm, we find that it allows us to reproduce the entire 4–5 μm spectrum very well, in particular the section from 4 to 4.3 μm, which is not well-produced by other line shapes. Our final retrieved temperature maps match closely those retrieved by *Grassi et al.* [2008] from the 4.3 to 5.1 μm range (excluding the CO band at 4.7 μm) who use a different sub-Lorentzian correction. Hence, the use of the *Tonkov et al.* [1996] line shape does not significantly effect our temperature retrievals, and allows us to better model the weak CO absorption feature. The *k*-tables were calculated on a grid with 20 temperatures spread equally between 100 and 350 K, and 20 pressure levels spread logarithmically between 4×10^{-8} and 2.7 bar, with a square spectral resolution of width 10 nm. When calculating spectra, NEMESIS convolved the output with a further square bin of width 10 nm, to achieve an effective instrument function close to that experimentally determined for VIRTIS-M.

[11] For these tests we assumed that the upper cloud optical depth was dominated by a lognormal distribution of H_2SO_4 droplets of mean radius of 1.0 μm and a variance of 1.29 (i.e., the mode 2 particles of *Grinspoon et al.* [1993]) and computed the extinction cross-section spectrum from Mie theory. Scattering effects were found to be negligible and so synthetic spectra were calculated assuming thermal emission only.

[12] Our first-guess, or a priori, temperature profile was taken from *Seiff* [1983], while for clouds we assumed the model of *Roos et al.* [1993], who used limb-darkening observations from Galileo/NIMS observations to determine that the mean cloud structure at equatorial latitudes was best matched by a cloud with a scale height of approximately 5.2 km. The a priori cloud profile density was thus set to decrease with height at this rate and the profile scaled to give a visible optical depth, at 630 nm, of 1.0 at an altitude of 65 km. For gaseous profiles the mole fraction of CO_2 was set to 0.965 [*von Zahn et al.*, 1983] and the remaining gases included were H_2O and SO_2, whose a priori profiles were set as recommended by *von Zahn et al.* [1983] and *Krasnopolskii and Parshev* [1983], although these gases were found to contribute negligibly to this spectral region. For CO we assumed a constant mole fraction with an a priori abundance of 100 ppm, based on determinations of the abundance in the lower atmosphere of 30 ppm (Tsang et al., submitted manuscript, 2008) and assuming the abundance increases with height.

[13] NEMESIS can simultaneously retrieve multiple variables and can model atmospheric constituents either as continuous or parameterized profiles. To assess the retrieval model and the validity of the correlated-*k* approximation [*Lacis and Oinas*, 1991], NEMESIS was first used to retrieve the vertical temperature profile alone from VIRTIS-M observations and the results compared with the temperature retrievals of *Grassi et al.* [2008]. Very good agreement was achieved, adding confidence to both retrieval models. In addition, we found that the effects of variable cloud opacity and temperature at altitudes less than 70 km were indistinguishable since the calculated extinction cross section of the assumed cloud particles has very little variation with wavelength across the 4–5 μm window.

[14] To investigate whether the CO abundance in Venus' mesosphere could indeed be retrieved from VIRTIS-M observations of Venus' night side from 4 to 5 μm, a series of retrieval tests was first undertaken whereby a set of synthetic spectra were generated from a set of randomly varied atmospheres. Synthetic Gaussian noise was added to these spectra, whose amplitude was set by the expected NESR of VIRTIS for typical observations. These synthetic 'measured' spectra were then fed into NEMESIS to retrieve some or all of the quantities varied and the retrieved properties compared with the values originally used to

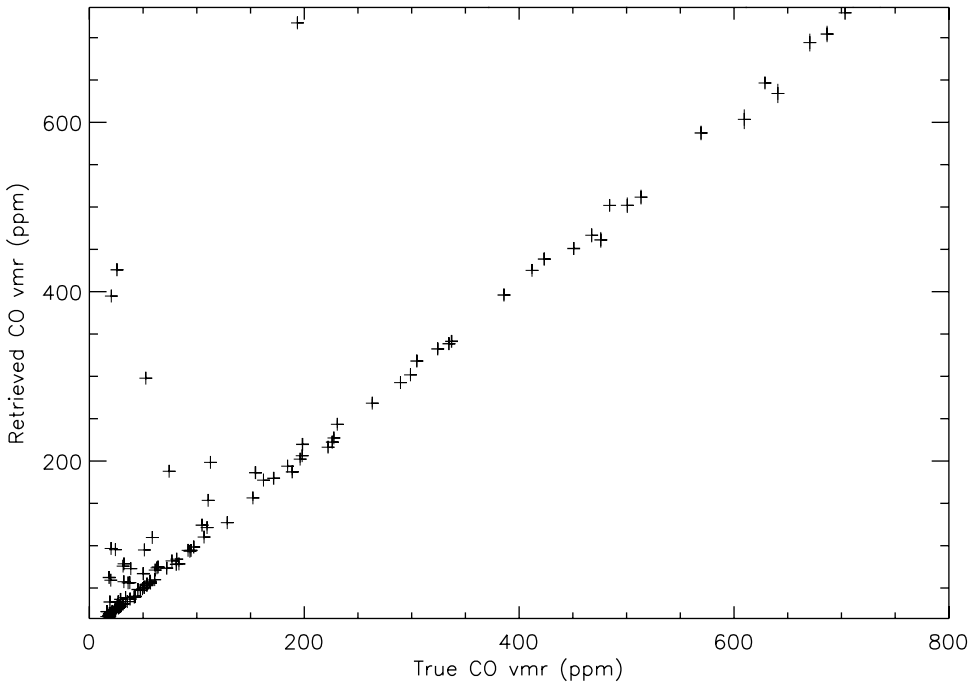

Figure 2. Correlation of retrieved CO with synthetic (or 'true') CO for the tests where temperature and mean CO abundance were retrieved with NEMESIS from synthetic spectra generated by randomly varying the temperature, mean CO abundance, and cloud opacity and scale height about their a priori values. The agreement between retrieved and 'true' CO can be seen to be very good. Cases where the retrieved CO is significantly greater than the true CO are cases where the cloud scale height exceeded 7 km.

generate the synthetic spectra. The error on the 'measured' spectra was taken to be the same NESR used to generate the random noise together with a degree of forward modeling error, which accounts for uncertainties in the line data and correlated-*k* approximation.

[15] Analysis of the spectrum generated from our a priori atmosphere showed that we are sensitive to the abundance of CO just about the cloud tops, whose lines usually appear in absorption as temperature falls with height at this altitude for most regions of the planet. Unfortunately, we found that these observations could reveal very little about the vertical distribution of CO and were thus forced to assume a vertical profile and decided to assume that the mole fraction varies little with height in this region, retrieving a single scaling factor.

[16] In the first test, the cloud profile was kept constant and a range of spectra generated by varying the temperature profile and CO mean mixing ratio. For the temperature profile, sine waves of temperature (varying with respect to height) were added to the a priori temperature profile with a random variation of phase, wavelength and amplitude. Similarly, the CO mean mixing ratio was varied randomly about the a priori value. NEMESIS then used the resulting synthetic spectra (to which Gaussian noise had been added) to retrieve the temperature profile and mean CO abundance, and the retrieved CO values were compared to the true values. In all cases the retrieved CO closely matched the 'true' CO values. However, we were concerned that variation in the cloud profile might be aliased as CO variations and so an additional set of test spectra was generated where temperature, CO and the cloud profile (represented by two parameters: (1) the integrated visible optical depth from space to an altitude of 65 km and (2) a scale height above and below that altitude) were randomly varied. These test spectra were then used (1) to again retrieve the temperature profile and mean CO mole fraction and (2) to retrieve the temperature profile, mean CO mole fraction and the two cloud parameters. In both cases the correlation between the retrieved and true CO was found to be very good (Figure 2) and can be explained by the fact that variations in the cloud profile produced spectral effects that are indistinguishable from thermal variations and also that we are most sensitive to CO just above the clouds. The cases in Figure 2 where the fitted CO greatly exceeded the true value were where the cloud scale height exceeded 7 km, which is a value far greater than anticipated for Venus, especially near the poles, where values of less than 5 km are expected. Hence, when analyzing the real observations, discussed in the next section, the cloud profile was kept fixed at its a priori profile and only the vertical temperature profile and mean CO mole fraction retrieved.

4. Retrievals

[17] Before analyzing the extended maps, the measurements in the VI0029 and VI0067 data sets, which had already been averaged into 20 × 20 pixel bins as described earlier, were further averaged by latitude into bins of width 10° and spaced every 5°, again to achieve Nyquist sampling. Since the Venus Express spacecraft was virtually over the south pole for both sets of observations, the emission

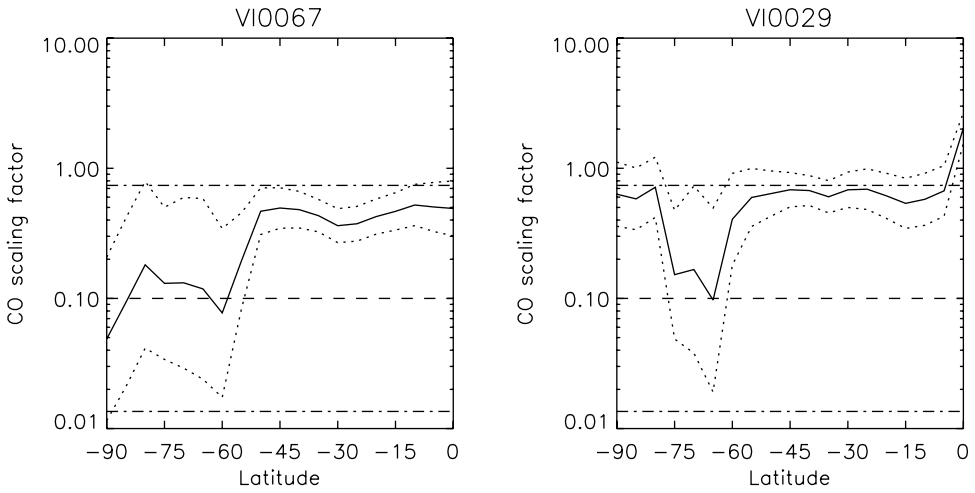

Figure 3. Variation of the retrieved CO volume mixing ratio scaling factor (of an assumed profile with 100 ppm CO at all altitudes) with latitude for the VI0067 and VI0029 observations. The horizontal dashed line indicates the a priori scaling factor and the dash-dotted lines indicate the a priori error limits. The retrieved CO abundance is indicated by the solid line, with retrieved error limits indicated by the dotted lines.

angle did not vary much with longitude and so the measured spectra could simply be averaged and a mean value of the emission angle assigned to each latitude bin. The a priori temperature profile was set as described earlier with an assumed temperature error of 10 K at all altitudes and a correlation length of 1.5 scale heights. For CO we initially assumed a scaling factor of 0.1 ± 0.2 of the a priori profile where the mole fraction was set to 100 ppm at all altitudes. To prevent the retrieved mole fraction ever going negative NEMESIS was set to retrieve the logarithm of the CO scaling factor.

[18] Figure 3 shows the variation of retrieved CO factor with latitude in the southern hemisphere for the VI0029 and VI0067 observations. It can be seen that in both cases at low latitudes the mean retrieved CO abundance is reasonably well constrained at a level of 40–50 ppm with an error of about 15 ppm. However, poleward of 50°S, the retrieved abundance drops rapidly to around 10 ppm, although the

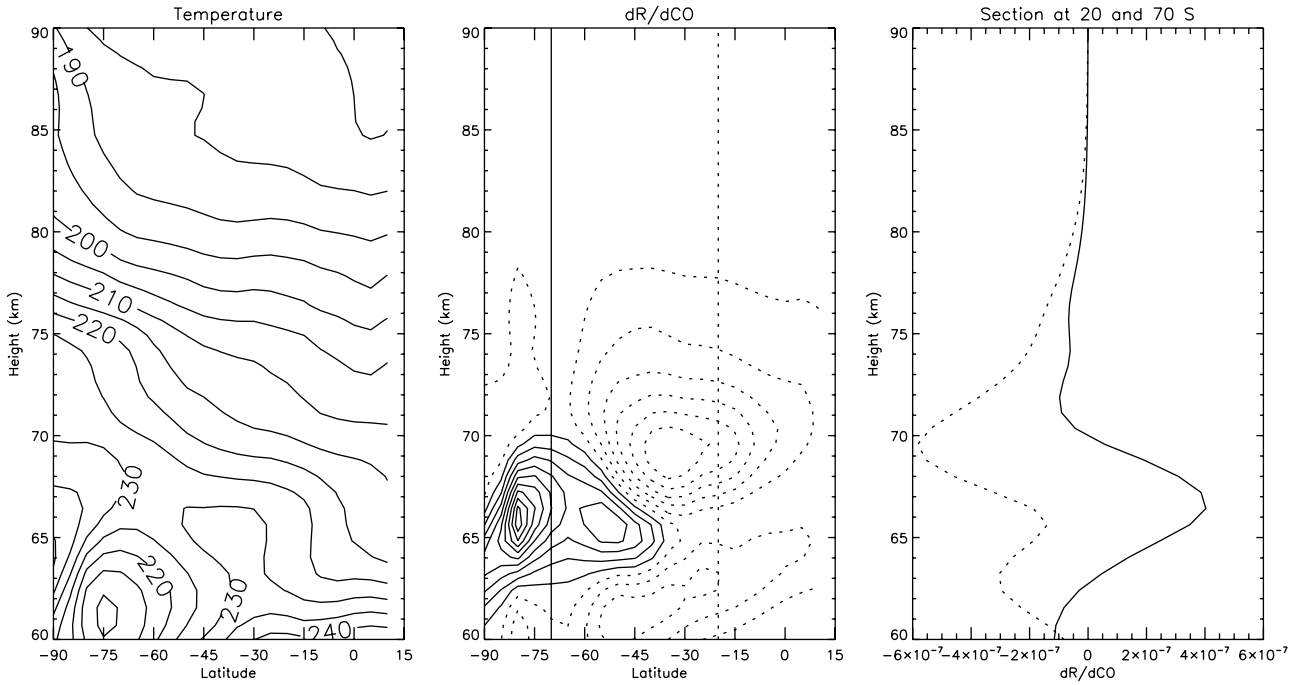

Figure 4. (left) Fitted temperature profile contour map, (middle) CO functional derivative (rate of change of mean radiance in the range 4–4.95 μm (μW cm^{-2} sr^{-1} μm^{-1}) with CO mole fraction) contour map, and (right) sections of the CO functional derivatives at 20°S (dotted line) and 70°S (solid line) for the combination of the VI0067 and VI0029 observations.

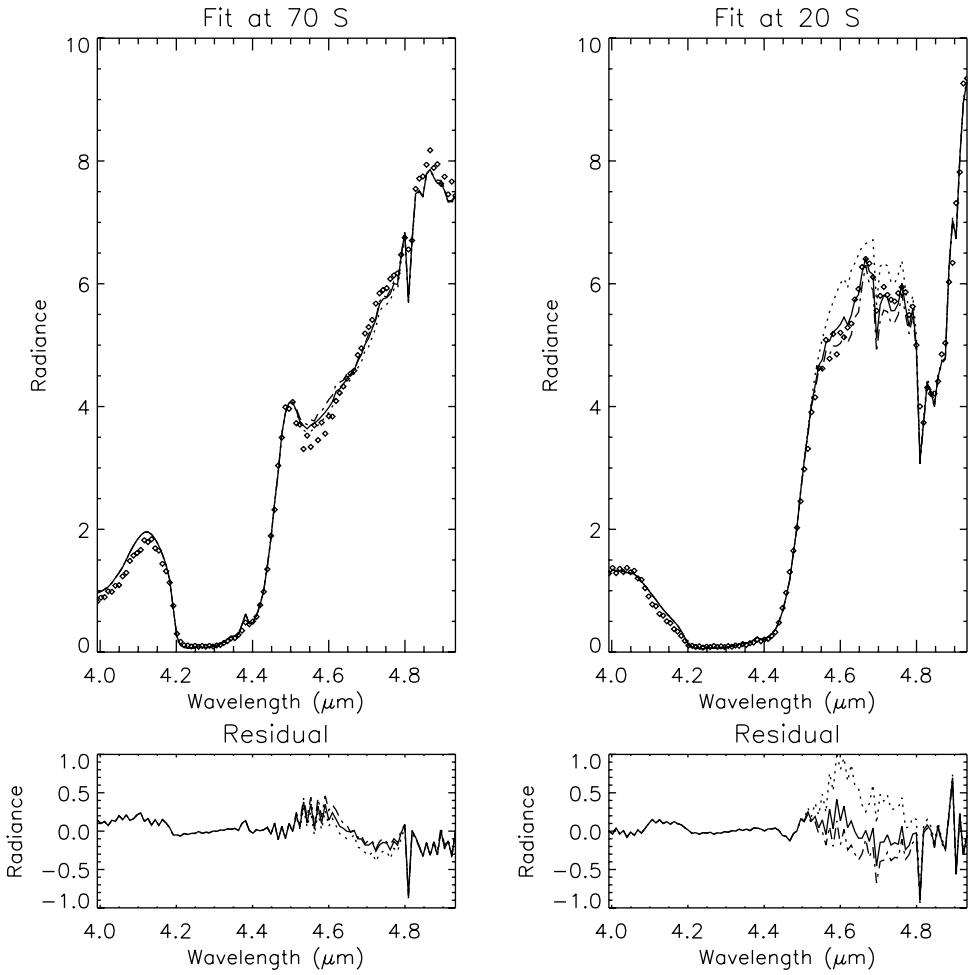

Figure 5. Quality of fit to the VI0067 observations at 20°S and 70°S. Measured spectra are shown as points and the units of radiance are μW cm^{-2} sr^{-1} μm^{-1}. Fitted spectra are shown by the solid lines. The spectrum calculated for the same temperature profile, but with 0 ppm of CO is shown as the dotted line, while the spectrum calculated for the same temperature profile, but with 100 ppm of CO is shown as the dash-dotted line. The top row compares the spectra, while the bottom row shows the residual difference between the measured and fitted spectra. The small absorption spike at 4.69 μm, which remains even for the 0 ppm CO case, is due to a weak Q-branch absorption of CO_2.

retrieved error increases markedly, approaching its a priori value, indicating the solution is poorly constrained by the measurements. Intriguingly, while Figure 3 shows the low value of CO extending to the pole for the VI0067 observations, the retrieved abundance for the VI0029 observations seems to increase toward the pole.

[19] To understand why the model has difficulty in retrieving a CO scaling factor in the polar collar around 70°S we need to look at the retrieved temperature profile, shown in Figure 4. From Figure 4 we can see that there is a marked temperature inversion in the 65–70 km altitude region at these latitudes associated with Venus' polar collar. Figure 4 also shows the CO functional derivative, that is to say the sensitivity of the calculated radiance (integrated over 4–4.95 μm) with respect to the CO abundance at all latitudes and altitudes, and sections are also shown at 20°S (typical midlatitude) and 70°S (in the middle of the polar collar). At 20°S we can see that the sensitivity to CO abundance is greatest at ~68 km and that increasing the CO fraction at all altitudes reduces the radiance, indicating the CO spectral lines to be in absorption. In contrast, at 70°S we can see that while the derivative of radiance with CO abundance is negative at some altitudes, it becomes positive in the temperature inversion region. Given that we can only retrieve a mean CO fraction from these measurements, having a situation where CO increases the mean radiance at some altitudes and reduces it at others leads to limited and ambiguous sensitivity to this species. As a test, we took the retrieved temperature profile and then recalculated the spectra assuming a CO abundance of (1) 0 ppm and (2) 100 ppm, shown in Figure 5, together with the spectrum calculated with the fitted CO value. In the region of the polar collar (70°S), very little difference between the spectra calculated with the retrieved CO abundance and the two trial abundances could be seen, whereas at midlatitudes (20°S) varying the mean CO abundance had a very clear effect on the spectra. Hence, while we can be reasonably confident of the retrieved CO abundance at low to mid latitudes, the abundance in the polar collar is effectively

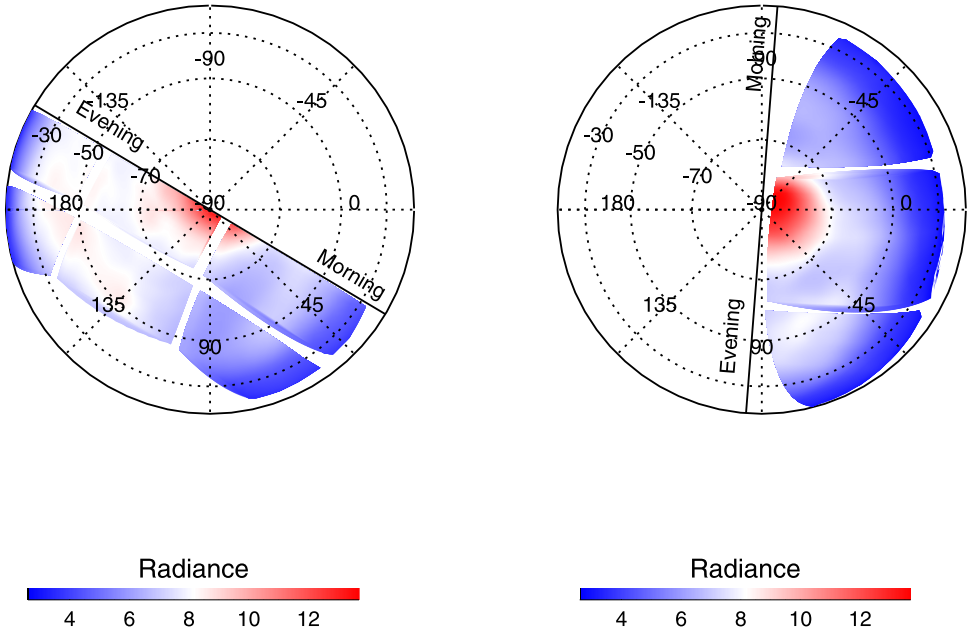

Figure 6. Measured radiance (in units of μW cm^{-2} sr^{-1} μm^{-1}) averaged over the range 4.8–5.0 μm for the (left) VI0067 and (right) VI0029 observations (binned into 20 × 20 pixel bins and stepped every 10 pixels in both directions).

unconstrained as is indicated by the retrieved errors differing little from the assumed a priori limits.

[20] As a final test, we also attempted to fit the observations with a temperature profile alone, keeping the CO value fixed at 100 ppm. We found that allowing the CO abundance to vary led to significantly improved fits to the observations in regions where we are sensitive to CO, showing that CO indeed has a significant and measurable effect on the observed spectrum.

[21] Having investigated the fitting of temperature and CO to the longitudinally averaged spectra, and determined at which latitudes CO might be retrieved, we then took the mapped observations and attempted to retrieve maps of the mean CO abundance in the southern hemisphere. Figure 6 shows the measured radiance (integrated from 4.8 to 5.0 μm) for the two sets of observations, indicating the position of the southern polar vortex and Figure 7 shows the precision to which the spectra could be fitted with our model expressed as $\frac{\chi^2}{n} = \frac{1}{n}\sum_{1}^{n}((m_i - s_i)/e_i)^2$, where m_i are the measured radiances of estimated error e_i, s_i are the calculated synthetic radiances, and n is the number of observations.

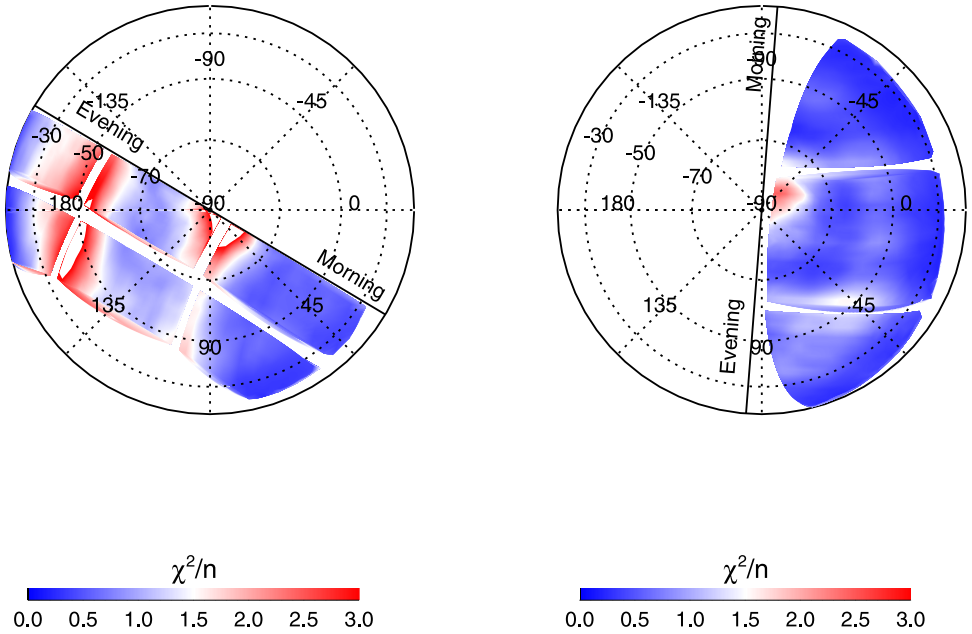

Figure 7. Fitted χ^2/n for the (left) VI0067 and (right) VI0029 observations.

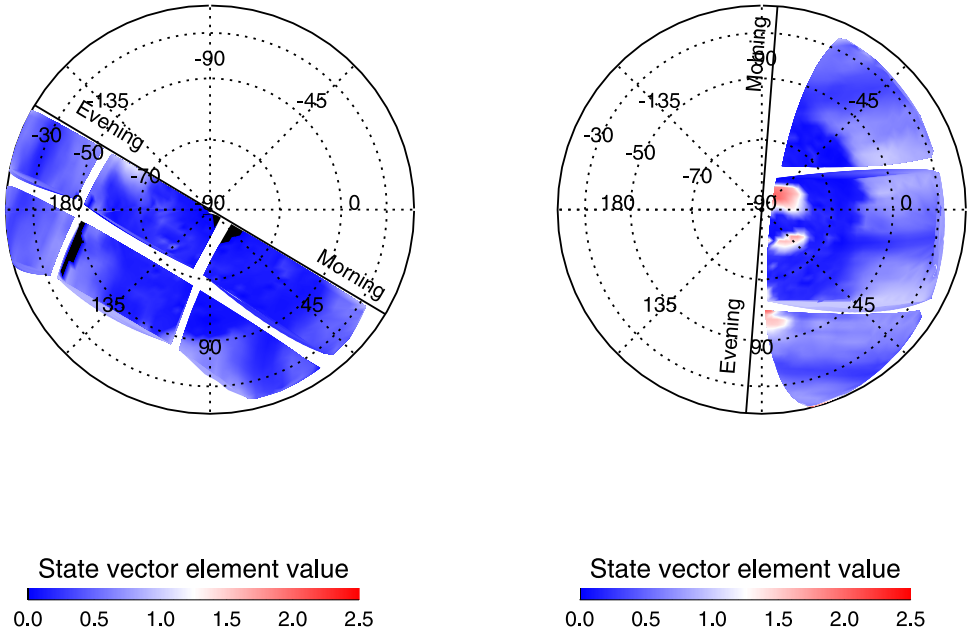

Figure 8. Retrieved CO scaling factor for the (left) VI0067 and (right) VI0029 observations, where areas with $\chi^2/n > 3$ have been masked (black areas). Note that a scaling factor of 1.0 corresponds to 100 ppm of CO.

Areas where χ^2/n is less than ~1 are regions where our model fits the observed spectra well and thus where we can have some confidence in our retrieved temperatures and CO abundances, if CO is detectable. Tests were conducted with a priori CO scaling factors of 1.0 ± 2.0, 0.1 ± 2.0 and 0.1 ± 0.2. In all cases very similar results were achieved since there is no trade-off to be made between vertical resolution and precision in these retrievals as the shape of the CO profile is fixed, resulting in a simple least squares solution for CO abundance that does not depend on the initial guess. Here we will show the results for the case where the CO a priori scaling factor was set to 0.1 ± 0.2. Since we fit the log of the scaling factor, it is important to remember that the a priori error assumed by NEMESIS was actually the fractional error in the abundance, in this case 2.0. In regions where there is little CO information, the retrieved fractional error remains close to 2.0, while in regions where CO is better constrained the fractional error reduces to less than 0.5. Figure 8 shows the retrieved CO factor regardless of retrieved error, while

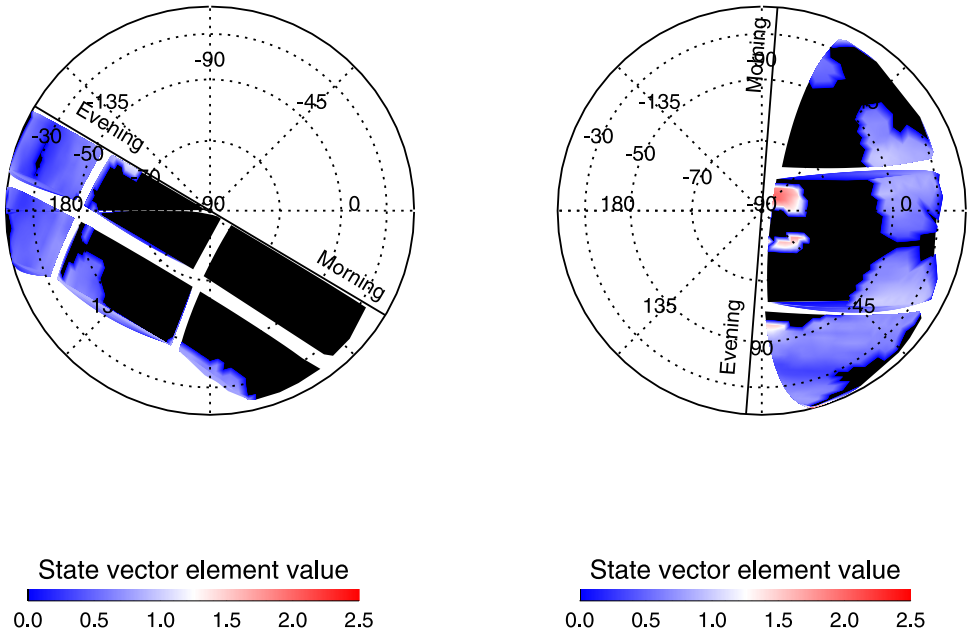

Figure 9. Fitted CO scaling factor for the (left) VI0067 and (right) VI0029 observations, where regions with a fractional error exceeding 0.4 and $\chi^2/n > 3$ have been masked.

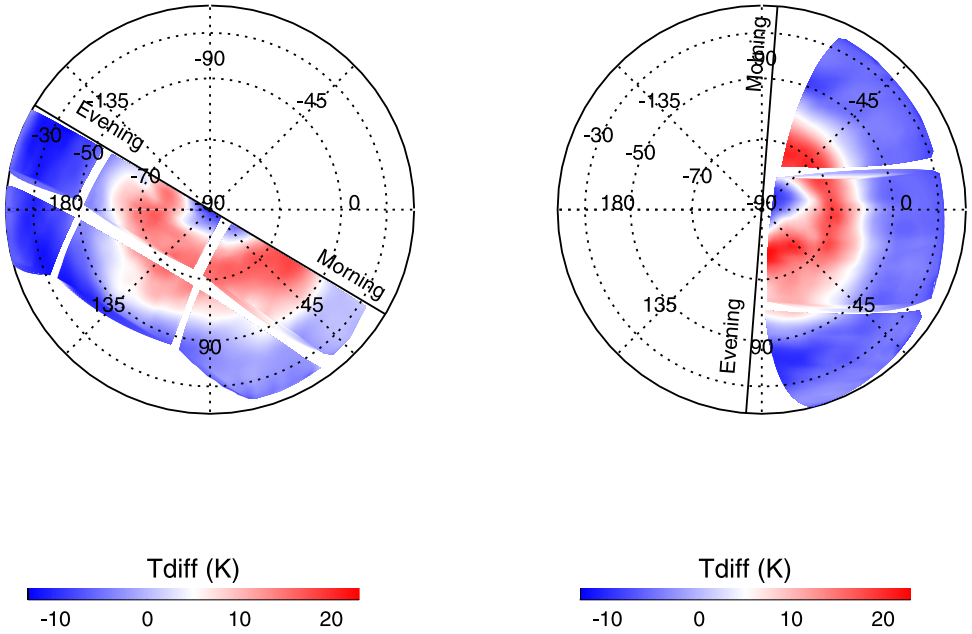

Figure 10. Retrieved values of T(70 km) − T(65 km) for the (left) VI0067 and (right) VI0029 observations, showing the inverted temperature profile at these altitudes over the polar collar.

Figure 9 shows the retrieved CO factor for cases where the fractional error has been reduced to less than 0.4 and thus where we can be confident that the CO abundance really is being constrained by the observations. The large black areas in Figure 9, mostly coincide with regions of the polar collar temperature inversion around 70°S, as shown in Figure 10.

[22] Comparing the retrieved CO maps of Figures 8 and 9 with the mean latitudinal variation for the two sets of observations shown earlier in Figure 3 we can see many of the same features: roughly constant CO abundance at low to mid latitudes, decreasing in the polar collar (but with much less constraint) and then increasing again toward the pole in the case of the VI0029 observations. Both maps seem to indicate a higher abundance of CO near the evening terminator at 50°S–70°S, although since the abundance of CO at similar latitudes on the morning terminator is not well constrained (as can be seen from Figure 9) owing to the vertical temperature structure there, it is not possible to determine if this is a real increase; it is possible that the CO

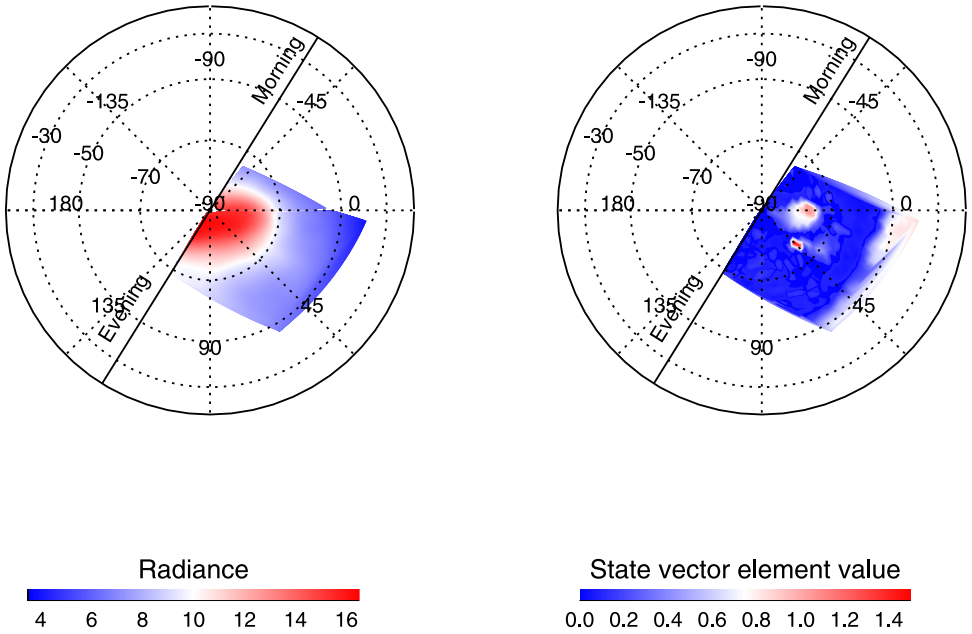

Figure 11. (left) Measured radiance (in units of μW cm^{-2} sr^{-1} μm^{-1}) averaged over the range 4.8–5.0 μm for the VI0038_00 observation, together with (right) the fitted CO abundance, again showing high CO over one of the two bright dipoles at 75°N, 0°E, indicative of rapid downwelling.

abundance is higher at all latitudes between 50°S and 70°S, but only observable near the evening terminator.

[23] The retrieved CO abundance near the pole for the VI0029 observation is particularly interesting as it seems to pick out high CO values over the polar dipole feature at 80°S, 45°E and 85°S, 45°W. This feature would appear to be absent in the VI0067 observation owing to the polar dipole being mostly on the day side in this case as indicated in Figure 6. To check if this was a repeatable feature, an additional observation, VI0038_00, which covers the south polar dipole, was analyzed in the same way to yield the fitted CO map shown in Figure 11. Again, we see high CO over one of the dipole hot spots at 75°N, 0°E, which would be consistent with this being a region of rapid downwelling dragging CO-rich air from higher altitudes to just above the cloud tops where it can be observed.

5. Discussion and Conclusions

[24] Observations of the (1–0) absorption band of CO at 4.7 μm on Venus' night side by the VIRTIS-M instrument of Venus Express have been used to investigate the spatial distribution of this gas above Venus' cloud tops. Retrieval tests showed the effects of cloud top temperature and cloud opacity to be indistinguishable in the 4–5 μm range and that the retrieved CO abundance differed little if clouds were included or omitted. Hence, the cloud opacity was fixed and a vertical temperature profile fitted simultaneously with the CO abundance.

[25] We find little spatial variation in the abundance of CO at midlatitudes, with a retrieved abundance of approximately 40 ± 10 ppm, a figure slightly higher than the levels observed by SPICAV/SOIR [*Svedhem et al.*, 2007] of 10–20 ppm at an altitude of 70 km. However, SPICAV/SOIR estimated the CO abundance at this altitude to decrease with height and as we are most sensitive to the abundance just above the cloud tops at ~65 km, our results are broadly consistent.

[26] Unfortunately, we find it very difficult to constrain the abundance of CO in the cold polar collar at 70°S as the retrieved temperature structure in the CO line-forming region masks the lines. However, the observations would suggest that CO increases toward the poles as we detect a significant signature of CO over Venus' south pole, coinciding with the areas of the bright dipole feature, which would be consistent with rapid downwelling in these features bringing CO-rich air from high altitudes to just above the clouds where it can be detected. In addition, both observations suggest the possibility of higher abundances of CO between 70°S and 50°S near Venus' evening terminator, although it is possible that this enhancement exists at all other longitudes, but cannot be detected owing to the CO lines being masked by the vertical temperature profile.

[27] A caveat to the conclusion of high CO over the polar dipole is that the shape of the vertical profile of CO had to be assumed in these retrievals, owing to the observations having effectively no vertical resolution assumption in the line forming region (65–70 km). It was assumed that the abundance of CO did not vary with altitude, but if the CO abundance actually decreases rapidly with altitude and if cloud tops in the polar dipole are much deeper than elsewhere, as is thought to be the case, then we would see a longer path length of CO in this region due simply to CO's vertical profile. However, since the polar dipole is thought to be a region of rapid downwelling and since we know the abundance of CO increases with height in the high atmosphere, where CO is formed by UV photolysis, it could be argued that this possibility is unlikely. To answer some of these questions and constrain the abundance of CO more closely will require more work and the analysis of many more observations than has been possible in this paper. One approach will be to analyze also the VIRTIS-H observations, which have much better spectral resolution, but poorer spatial sampling. This work is currently in progress, but the results are not yet mature enough to be presented here. In addition, limb observations would allow us to directly determine the vertical profile of CO above the cloud tops around the planet and help greatly to resolve any possible temperature/cloud ambiguities and we hope that such measurements can be conducted by VIRTIS during the remainder of its mission.

[28] **Acknowledgments.** The Venus Express/VIRTIS team is acknowledged for their work. This research was made possible by funding from the United Kingdom Science and Technology Facilities Council.

References

Bertaux, J.-L., et al. (2007), A warm layer in Venus' cryosphere and high altitude measurements of HF, HCl, H_2O and HDO, *Nature*, *450*, 646–649, doi:10.1038/nature05974.

Bézard, B., C. de Bergh, D. Crisp, and J. Maillard (1990), The deep atmosphere of Venus revealed by high-resolution night side spectra, *Nature*, *345*, 508–511, doi:10.1038/345508a0.

Clancy, R. T., and D. O. Muhleman (1991), Long-term (1979–1990) changes in the thermal, dynamical and compositional structure of the Venus mesosphere as inferred from microwave spectral line observations of ^{12}CO, ^{13}CO, and $C^{18}O$, *Icarus*, *89*, 129–146, doi:10.1016/0019-1035(91)90093-9.

Clancy, R. T., B. J. Sandor, and G. H. Moriarty-Schieven (2003), Observational definition of the Venus mesopause: Vertical structure, diurnal variation, and temporal instability, *Icarus*, *161*, 1–16, doi:10.1016/S0019-1035(02)00022-2.

Collard, A., F. Taylor, S. Calcutt, R. Carlson, L. Kamp, and K. Baines (1993), Latitudinal distribution of carbon monoxide in the deep atmosphere of Venus, *Planet. Space Sci.*, *41*, 487–494, doi:10.1016/0032-0633(93)90031-V.

Conrath, B. J., P. J. Gierasch, and E. A. Ustinov (1998), Thermal structure and para hydrogen fraction in the outer planets from Voyager IRIS measurements, *Icarus*, *135*, 501–517, doi:10.1006/icar.1998.6000.

de Bergh, C., V. I. Moroz, F. W. Taylor, D. Crisp, B. Bezard, and L. V. Zasova (2006), The composition of the atmosphere of Venus below 100 km altitude: An overview, *Planet. Space Sci.*, *54*, 1389–1397, doi:10.1016/j.pss.2006.04.020.

Grassi, D., P. Drossart, G. Piccioni, N. I. Ignatiev, L. V. Zasova, A. Adriani, M. L. Moriconi, P. G. J. Irwin, A. Negrao, and A. Migliorini (2008), Retrieval of air temperature profiles in the Venusian Mesosphere from VIRTIS-M data: Description and validation of algorithms, *J. Geophys. Res.*, doi:10.1029/2008JE003075, in press.

Grinspoon, D. H., J. B. Pollack, B. R. Sitton, R. W. Carlson, L. W. Kamp, K. H. Baines, T. Encrenaz, and F. W. Taylor (1993), Probing Venus's cloud structure with Galileo NIMS, *Planet. Space Sci.*, *41*, 515–542, doi:10.1016/0032-0633(93)90034-Y.

Gurwell, M. A., D. O. Muhleman, K. P. Shah, G. L. Berge, D. J. Rudy, and A. W. Grossman (1995), Observations of the CO bulge on Venus and implications for mesospheric winds, *Icarus*, *115*, 141–158, doi:10.1006/icar.1995.1085.

Hanel, R. A., B. J. Conrath, D. E. Jennings, and R. E. Samuelson (2003), *Exploration of the Solar System by Infrared Remote Sensing*, 2nd ed., Cambridge Univ. Press, Cambridge, U. K.

Hong, Y., and B. Fegley (1997), Formation of carbonyl sulfide (OCS) from carbon monoxide and sulfur vapor and applications to Venus, *Icarus*, *130*, 495–504, doi:10.1006/icar.1997.5824.

Huebner, W. F., J. J. Keady, and S. P. Lyon (1992), Solar photo rates for planetary atmospheres and atmospheric pollutants, *Astrophys. Space Sci.*, *195*, 1–289, 291–294.

Irwin, P. G. J., N. A. Teanby, R. de Kok, L. N. Fletcher, C. J. A. Howett, C. C. C. Tsang, C. F. Wilson, S. B. Calcutt, C. A. Nixon, and P. D. Parrish (2008), The NEMESIS planetary atmosphere radiative transfer and retrieval tool, *J. Quant. Spectrosc. Radiat. Transf.*, *109*, 1136–1150, doi:10.1016/j.jqsrt.2007.11.006.

Krasnopolskii, V. A., and V. A. Parshev (1983), Photochemistry of the Venus atmosphere, in *Venus*, pp. 431–458, Univ. of Ariz. Press, Tucson.

Lacis, A. A., and V. Oinas (1991), A description of the correlated-*k* distribution method for modeling nongray gaseous absorption, thermal emission, and multiple scattering in vertically inhomogeneous atmospheres, *J. Geophys. Res.*, *96*, 9027–9063, doi:10.1029/90JD01945.

Mills, F. P., and M. Allen (2007), A review of selected issues concerning the chemistry in Venus' middle atmosphere, *Planet. Space Sci.*, *55*, 1729–1740, doi:10.1016/j.pss.2007.01.012.

Pollack, J., J. Dalton, D. Grinspoon, R. Wattson, R. Freedman, D. Crisp, D. Allen, B. Bezard, C. de Bergh, and L. Giver (1993), Near-infrared light from Venus' night side: A spectroscopic analysis, *Icarus*, *103*, 1–42, doi:10.1006/icar.1993.1055.

Rodgers, C. D. (2000), *Inverse Methods for Atmospheric Sounding: Theory and Practice*, World Sci., Hackensack, N. J.

Roos, M., P. Drossart, T. Encrenaz, E. Lellouch, B. Bezard, R. W. Carlson, K. H. Baines, L. W. Kamp, F. W. Taylor, and A. D. Collard (1993), The upper clouds of Venus: Determination of the scale height from NIMS-Galileo infrared data, *Planet. Space Sci.*, *41*, 505–514, doi:10.1016/0032-0633(93)90033-X.

Rothman, L. S., et al. (2005), The HITRAN 2004 molecular spectroscopic database, *J. Quant. Spectrosc. Radiat. Transf.*, *96*, 139–204, doi:10.1016/j.jqsrt.2004.10.008.

Seiff, A. (1983), Thermal structure of the atmosphere of Venus, in *Venus*, pp. 215–279, Univ. of Ariz. Press, Tucson.

Svedhem, H., D. V. Titov, F. W. Taylor, and O. Witasse (2007), Venus as a more Earth-like planet, *Nature*, *450*, 629–632, doi:10.1038/nature06432.

Tonkov, M., N. Filippov, V. Bertsev, J. Bouanich, V.-T. Nguyen, C. Brodbeck, J. Hartmann, C. Boulet, and F. Thibault (1996), Measurements and empirical modeling of pure CO_2 absorption in the 2.3 μm region at room temperature: Far wings, allowed and collision-induced bands, *Appl. Opt.*, *35*, 4863–4870.

von Zahn, U., S. Kumar, H. Niemann, and R. Prinn (1983), Composition of the Venus Atmosphere, in *Venus*, pp. 299–430, Univ. of Ariz. Press, Tucson.

R. de Kok, P. G. J. Irwin, F. W. Taylor, C. C. C. Tsang, and C. F. Wilson, Atmospheric, Oceanic, and Planetary Physics, Clarendon Laboratory, University of Oxford, Parks Road, Oxford OX1 3PU, UK. (irwin@atm.ox.ac.uk)

P. Drossart, LESIA, Observatoire de Paris, 5 place Jules Janssen, F-92195 Meudon, France.

D. Grassi and A. Negrão, INAF-IFSI, Via del Fosso del Cavaliere, 100, I-00133 Rome, Italy.

G. Piccioni, INAF-IASF, Via del Fosso del Cavaliere, 100, I-00133 Rome, Italy.